

## SCALED-UP NONEQUILIBRIUM AIR PLASMAS

Zdenko Machala<sup>\*</sup>, Christophe O. Laux<sup>†</sup>, Xavier Duten<sup>‡</sup>, Denis M. Packan<sup>§</sup>, Lan Yu<sup>\*\*</sup>, Charles H. Kruger<sup>††</sup>

*Thermosciences Division, Mechanical Engineering Department  
Stanford University, Stanford, CA 94305*

### Abstract

The volume scalability of nonequilibrium plasmas produced by electrical discharges in atmospheric pressure air has been investigated. A variety of direct current (DC) and pulsed glow discharges obtained in either slow flow of ambient or fast flow of preheated (~2000 K) air at atmospheric pressure is presented. Single DC and repetitively pulsed discharges represent the first approach. Stable discharges with electron number densities as high as  $10^{12} \text{ cm}^{-3}$  were obtained without filamentation. A large decrease of the input power by 2-3 orders of magnitude was achieved in pulsed discharges, in comparison with the DC discharges. A dual-discharge facility was developed that combines two parallel DC discharges in either ambient or preheated air. Uniform plasma volumes of a few cubic centimeters have been achieved by this technique. Multiple pulsed discharges in parallel have been examined as well in order to increase the plasma volume. Finally, some paradoxical results on DC discharges in transverse gas flow are presented. The temperature distribution effecting the reduced electric field  $E/N$  is found to strongly influence the shape of the discharge.

### 1. Introduction

Large volume air plasmas at atmospheric pressure present considerable interest for a wide range of applications, such as electromagnetic wave shielding, air pollution control, material processing, surface treatment, and biochemical decontamination. Each application has, of course, its specific requirements for plasma properties. Generally speaking, desirable conditions are electron densities of the order of  $10^{12}$ - $10^{13} \text{ cm}^{-3}$  and gas temperatures below 2000 K. Our research focuses on glow discharges at atmospheric pressure. These discharges have received renewed attention during the past few years.<sup>1-18</sup>

Two main difficulties in the research on glow discharges at atmospheric pressure have been encountered, the power required to maintain such plasmas at atmospheric pressure, as well as their size. The power required to sustain the plasma with direct-current (DC) discharges is large ( $3 \text{ kW/cm}^3$  for  $10^{12} \text{ electrons/cm}^3$ ). However, a drastic reduction of the power required to

sustain the same electron number density can be obtained by the use of a repetitively pulsed discharge. The power requirements of the repetitively pulsed discharge were measured to be  $12 \text{ W/cm}^3$ , a factor 250 times lower than with the DC discharge.<sup>7-9</sup>

The goal of this study is the scalability of nonequilibrium air discharges at atmospheric pressure. Section 2 describes the experimental facilities and measurement techniques. Section 3 provides an overview of experiments with single DC and repetitively pulsed discharges in both ambient (room temperature) and preheated flows of air at atmospheric pressure. Section 4 describes the dual-discharge scalability studies with ambient temperature and preheated air flows. Section 5 presents studies of multiple parallel pulsed discharges. Finally, section 6 presents a study of DC discharges in transverse preheated air flow.

---

\* Postdoctoral Fellow, Member AIAA

† Senior Research Scientist, Associate Fellow AIAA, currently Professor, Ecole Centrale Paris, France

‡ Postdoctoral Fellow, currently Professor, University Paris-Nord, France

§ Graduate Research Assistant, Student Member AIAA, currently Postdoctoral Fellow, ONERA, France

\*\* Postdoctoral Fellow

†† Professor, Vice Provost, Dean of Research and Graduate Policy, Member AIAA

## 2. Experimental Facilities

### 2.1. Microwave Plasma Torch

Experiments with DC and pulsed discharges were conducted in ambient and preheated air at atmospheric pressure. We preheat air to about 2000 K with a microwave plasma torch (Litmas Red) powered by a 5 kW magnetron (Richardson Electronics switching power generator Model SM1050). The torch has a maximum power output of 3 kW. The temperature and velocity of the outgoing plasma can be set by varying the power output and gas flow rate, as well as by using water-cooled test sections and nozzles. The torch is able to generate air plasmas in the temperature range 750-4700 K at flow velocities from 20 to 200 m/s, corresponding to gas flow rates from 8 to 110 slpm (standard liters per minute). The microwave torch head and a close-up view of the air plasma plume at typical experimental conditions ( $T \sim 2000$  K,  $v \sim 160$  m/s) are shown in Figure 1.

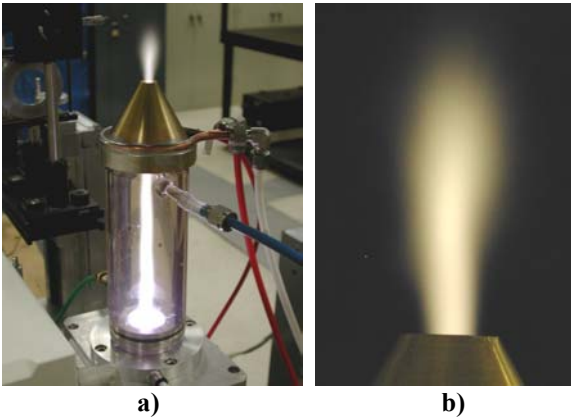


**Figure 1.** a) Microwave plasma torch head, test-section and accelerating nozzle with the exit diameter 1 cm. b) Air plasma plume at the exit of the nozzle,  $T \sim 2000$  K,  $v \sim 160$  m/s.

### 2.2. Optical Diagnostics

Temperature and electron number density measurements were made by spatially resolved optical emission spectroscopy. Spectra of the 2<sup>nd</sup> positive system of  $N_2$  ( $C^3\Pi_u - B^3\Pi_g$  transition) were used to determine the rotational and vibrational temperatures  $T_r$  and  $T_v$ , respectively, using the NEQAIR2 radiation code<sup>19</sup>.

In atmospheric pressure plasmas,  $T_r$  is close to the gas temperature  $T$ .

The optical set-up is shown in Figure 2. Light collected with two magnesium fluoride lenses is focused onto a fiber optic connected to an Ocean Optics Model S2000 dual spectrometer, fitted with two grating/CCD combinations. The two 1200 and 600 grooves/mm gratings provide coverage of the spectral ranges 200-500 nm, and 400-1100 nm. The optical train is mounted on a translation stage, which enables lateral scanning capability. Absolute intensity calibrations were obtained by means of two radiance standards traceable to NIST calibrations.

## 3. Review of Experiments with Single Discharges

Single DC and pulsed glow discharges in air and nitrogen at atmospheric pressure have been extensively studied at Stanford University over the past few years, both experimentally and theoretically.<sup>1-12</sup> The objective of these studies was to provide a clear understanding of the mechanisms of ionization and recombination in atmospheric pressure air plasmas.

Spatially and temporally resolved diagnostics, including quantitative Optical Emission Spectroscopy (OES) and Cavity Ring-Down Spectroscopy (CRDS), as well as electrical techniques, have been developed to measure the electron number density and the gas temperature in these discharges.<sup>3, 6, 9, 11</sup>

The DC and pulsed discharges are typically applied between two platinum pins parallel to the axis of the gas flow. The pins are welded onto cooled stainless steel tubes in order to prevent their melting at the elevated temperature operation. Although the platinum pins are not required to operate the discharge, they help stabilize the discharge spatially.

### 3.1. DC Discharges in Ambient Air

Atmospheric glow DC discharges are obtained by applying a few hundred volts to a few kilovolts between ballasted electrodes. A 15 kW DC power supply, Del High Voltage Model RHVS, capable of delivering up to 10 kV and 1.5 A, is employed, together with a ballast resistor of 3-50 k $\Omega$  (typically 18 k $\Omega$ ) in series with the discharge, as shown in Figure 2.

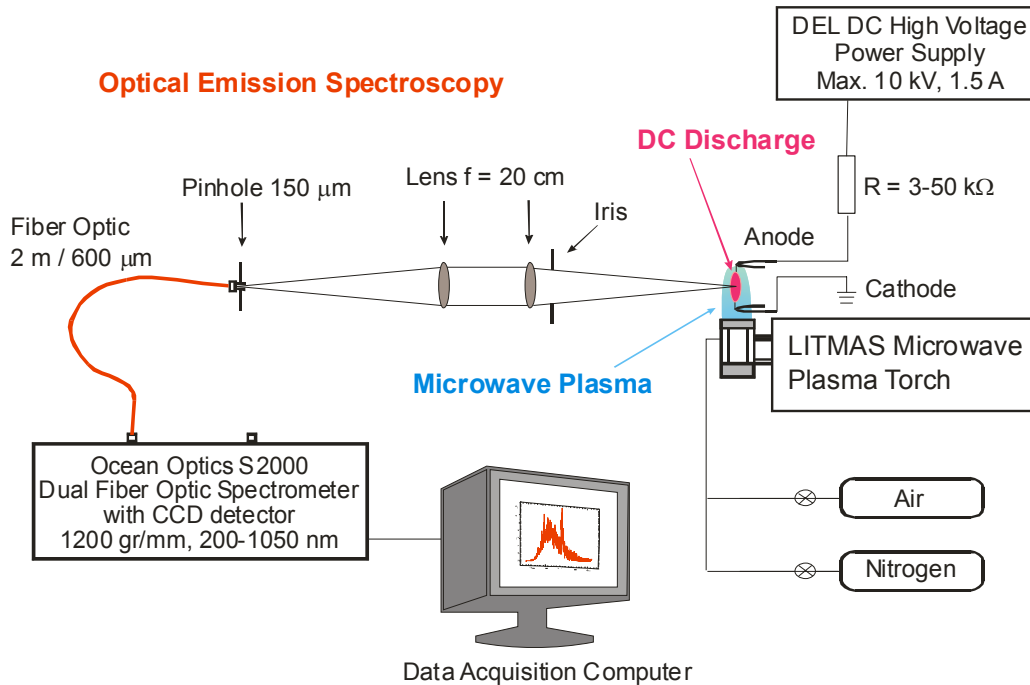


**Figure 2. Overall view of the experimental setup for DC discharges.**

Figure 3a shows the picture of a typical DC glow discharge in **ambient air** at atmospheric pressure. A DC glow discharge in nitrogen at the same conditions is also shown for comparison (Figure 3b). The gas (either air or nitrogen) is injected at about 0.5 m/s between two electrodes separated by 1.2 cm. The air discharge voltage and current are 1.5 kV and 20 mA, respectively. The stratification into dark and bright layers typical of low pressure glow discharges is also observed at atmospheric pressure, especially at currents below 20 mA. Note for instance the Faraday dark space near the cathode (lower electrode) in the nitrogen discharge (Figure 3b) Nevertheless, the cathode layers are concentrated in the immediate vicinity of the cathode, thus suggesting that the positive column occupies most of the interelectrode space. This observation was confirmed by electrical measurements. The electric field is found to be uniform and equal to approximately 935 V/cm in the interelectrode space, except within the 1 mm region close to the cathode. The voltage drop across the cathode region is about 280 V, a value typical of the cathode fall in air glow discharges with Pt electrodes.<sup>20</sup>

The diameter of the discharge in air measured by emission spectroscopy of the  $N_2$   $C^3\Pi_u-B^3\Pi_g$  (0,0) transition at 337 nm is approximately 1.7 mm for the current of 20 mA. The same discharge diameter was measured for the nitrogen discharge of the same conditions. Since the C state of  $N_2$  is produced by electron-

impact excitation, this diameter is representative of the region with high electron number density. In Figure 3, the discharge in air appears to be wider than the discharge in nitrogen. This effect is due to the presence of a halo around the discharge produced by  $NO_2$  emission in the surrounding air environment heated by the discharge. The measured gas temperature in the discharge channel at these conditions is about 2000 K, and the estimated electron temperature is around 9500 K. This thermal nonequilibrium provides further indication that the discharge is a glow and not an arc.

The DC glow discharges in ambient air flows can be operated in the current range 2-200 mA. The corresponding gas temperatures, measured by optical emission spectroscopy at the centerline of the discharge column, are in the range 1500-4000 K, and depend strongly on the gas velocity. The current-voltage characteristics of the discharge is descending. The gap length can be varied up to 10 cm, depending on the flow velocity of the gas and the discharge current. Plasma volumes of  $\sim 0.5$  cm<sup>3</sup> can be produced in this manner.

The conductivity, hence the electron number density, can be obtained using Ohm's law and the measured electric field strength and current density (determined from the measured discharge current and discharge diameter). We estimated the electron number density  $n_e$  to be approximately  $10^{12}$  cm<sup>-3</sup>. This value agrees well with the  $n_e$  measured by Cavity Ring-Down

Spectroscopy of  $N_2^+$ , the dominant ion in nitrogen glow discharges.<sup>11</sup>

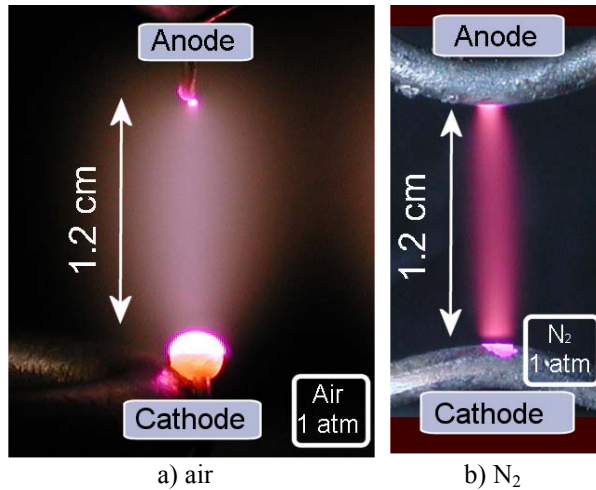


**Figure 3. DC glow discharge in a) air and b) nitrogen flow ( $v = 0.5$  m/s) at room temperature and atmospheric pressure.  $I = 20$  mA,  $U = 1.5$  kV in air, 1.4 kV in  $N_2$ .**

### 3.2. DC Discharges in Fast Flow of Preheated Air

DC discharge experiments were also conducted with fast flowing **preheated air** at  $\sim 2000$  K. The main reason for going to fast gas flows (20-400 m/s) is that discharges at slow flows result in significant gas heating, especially at high currents where electron number densities of  $10^{12}$   $cm^{-3}$  or higher are achieved. The mechanism of gas heating can be explained as follows.

In the DC discharges, a large fraction of the electron energy is lost via excitation of the vibrational modes of air molecules, mainly  $N_2$ . These vibrational modes subsequently relax through collisions with the dominant species, i.e. O,  $N_2$ , and  $O_2$ . This collisional quenching transfers the energy from vibration into the translational modes of molecules, which results in Joule heating of the gas. This process is called vibrational-translational energy transfer (VT transfer). In slow air flows, the residence time of the gas in the discharge is long enough to enable the VT transfer. As a result, the gas is heated.

In fast air flows, on the other hand, the vibrational modes of  $N_2$  have shorter time to relax, hence cannot heat the gas as much over the short residence time between the two electrodes. Thus the temperature in the discharge is almost determined by the inlet gas flow. Yet, it is very difficult to maintain stable DC discharges in fast flows of ambient air. This is because electron attachment is fast, whereas ionization is slow

since the reduced field strength  $E/N$  (where  $E$  is the field strength and  $N$  is the gas density) is lower due to the lower gas temperature, hence higher  $N$ .

For these reasons, we used a fast flow of preheated air at  $\sim 2000$  K. At this temperature, electron attachment does not play an important role. Moreover, the density is about seven times lower than at room temperature and the reduced field strength  $E/N$  is sufficient to maintain the discharge. When the residence time of the flow in the discharge column is shorter than the characteristic time for VT relaxation, the temperature remains close to 2000 K.

Both DC and repetitively pulsed discharges were examined. In these experiments, the preheated air streams were generated by a 50 kW inductively coupled plasma torch described in detail elsewhere.<sup>1</sup>

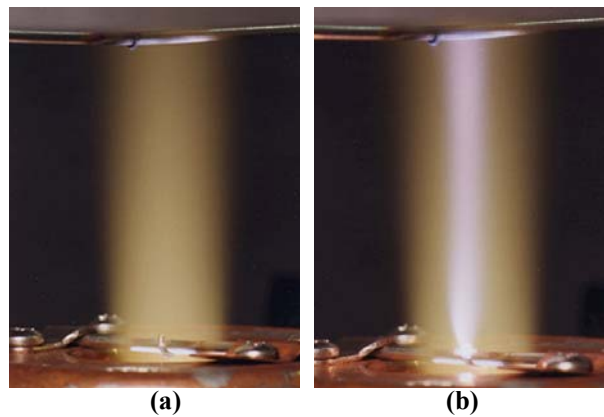


**Figure 4. Air plasma at 2000 K a) without discharge, b) with discharge (1.4 kV/cm, 200 mA). Interelectrode gap 3.5 cm.**

Figure 4 shows photographs of an air plasma plume preheated to 2000 K (Figure 4a) and of the same plume with a DC discharge applied (Figure 4b). In these experiments, the interelectrode distance is about 3.5 cm, and the discharge diameter measured by the emission of the  $N_2$  C-B transition is 3.2 mm. The discharge diameter is larger in preheated air than in ambient air, by approximately a factor of two. This effect is due to the presence of larger dissipative thermal gradients in the ambient air discharge than in the preheated air plume.

### 3.3. Repetitively Pulsed Discharge in Preheated Air

As the power required to sustain elevated electron densities with DC discharges is large, a power reduction strategy based on pulsed electron heating was explored.<sup>7-10</sup> This strategy is illustrated in Figure 5. Short (10 ns) high voltage pulses (10 kV) are applied to increase the electron number density. After each pulse

$n_e$  decreases according to electron recombination processes. When  $n_e$  reaches the minimum desired value, the next pulse is applied. The average electron density obtained with this method depends on the pulse duration, pulse voltage, and the interval between pulses.

A repetitive pulser capable of generating 10 ns pulses, with peak voltages of 3-12 kV and pulse repetition frequencies up to 100 kHz from Moose-Hill/FID Technologies was used. The electric circuit and the pulser are described elsewhere.<sup>7, 9, 10</sup> The discharge is applied in preheated air at atmospheric pressure and about 2000 K. The power deposited into the plasma by the discharge was determined from the pulse current (measured with a Rogowski coil), the voltage between the electrodes minus the cathode potential fall, and the measured discharge diameter.

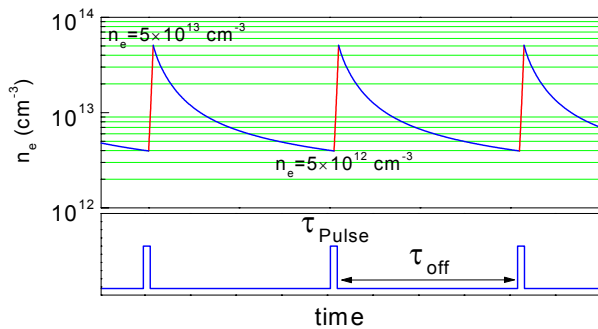


Figure 5. Repetitively pulsed strategy.

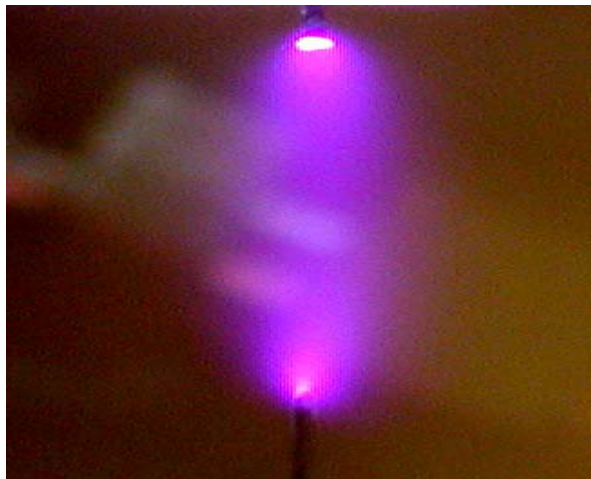


Figure 6. Photograph of 10 ns, 100 kHz repetitively pulsed discharge in preheated air at 2000 K and 1 atm. Interelectrode distance 1.2 cm. Discharge diameter 3.2 mm.

Figure 6 shows a picture of the repetitively pulsed discharge in preheated air at 2000 K. Here the

interelectrode distance is 1.2 cm, and the discharge diameter is about 3.2 mm, which is comparable to the diameter of the DC discharge. The measured electron number density varies from  $7 \times 10^{11}$  to  $1.7 \times 10^{12}$   $\text{cm}^{-3}$ , with an average value of about  $10^{12}$   $\text{cm}^{-3}$ . The power deposited into the discharge is measured to be  $12 \text{ W/cm}^3$ , consistent with the theoretical value of  $9 \text{ W/cm}^3$  for an optimized pulsed discharge producing  $10^{12}$  electrons/ $\text{cm}^3$ .<sup>9</sup> It is lower, by a factor of 250, than the power of  $3 \text{ kW/cm}^3$  required to sustain  $10^{12}$  electrons/ $\text{cm}^3$  with a DC discharge. More details about these experiments and modeling can be found elsewhere.<sup>7-10</sup>

#### 4. Dual-Discharge Experiments

Experiments have been conducted to combine two discharges operating in parallel in order to increase the volume of the plasma, and to investigate scaling effects.

The electric circuit used to generate dual-discharges at atmospheric pressure is shown in Figure 7. To stabilize the discharges, each cathode and anode is ballasted separately by a  $3 \text{ k}\Omega$  water-cooled Khan-tal-Globar resistor. Ambient air is injected with typical flow rates of 100 slpm, corresponding to a gas velocity of 50 cm/s at room temperature, through a 7 cm diameter flow straightener, used to stabilize the incoming flow. In experiments with preheated fast air flow, the dual-discharge facility is placed directly above the exit of the microwave torch nozzle. 2D translation stages are used to vary the lateral distance between the two discharges.

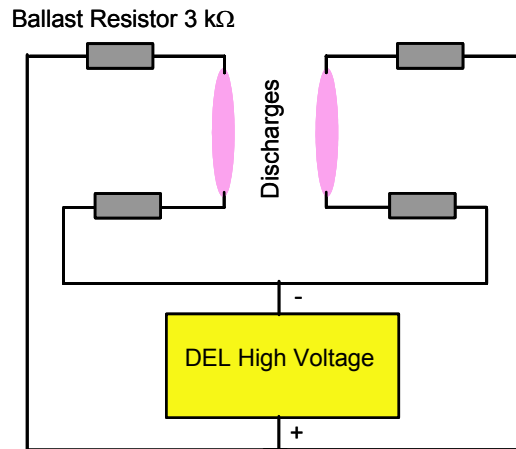


Figure 7. Electric circuit for dual DC discharge experiments

#### **4.1. Dual-Discharges in Ambient Air**

Figure 8 shows photographs of a dual DC discharge as a function of the inter-discharge spacing. The working gas is air at atmospheric pressure, injected into the discharge at a flow velocity of about 50 cm/s. The interelectrode distance is kept fixed at 1.2 cm, while the lateral distance  $l$  between the two discharges is decreased from 1.35 to 0.85 cm. In all cases, the voltage and current are 1.4 kV and 200 mA (~100 mA per single discharge).

For  $l = 1.35$  cm, the two discharges are clearly separated. When the lateral distance is decreased to 1.15 cm, the space between the two discharges becomes gradually filled with a plasma “cloud”. This luminous halo is due to the  $\text{NO}_2$  emission of the surrounding air environment heated by the discharge. Thus, as the lateral distance decreases, the temperature in the region between the two discharges increases due to heat transfer, leading to an increase of the size of the halo. At lateral distances smaller than 1.05 cm, the two discharges merge into a single one.

Measurements of the emission intensity of the  $\text{N}_2$  C-B (0,0) band head were also performed to determine the diameter of the central part of the discharge. For this purpose, an intensified CCD camera (Roper Scientific PI-MAX1024), coupled with a bandpass filter centered around the  $\text{N}_2$  C-B (0,0) band head (337 nm) was used. Results are presented in Figure 9. The experimental conditions are the same as those reported on Figure 8. The measured FWHM of  $\text{N}_2$  C-B (0,0) band head emission at mid-distance between the electrodes is approximately 1.3 mm when the two discharges are separated ( $l \geq 1$  cm), and increases to 2 mm when the lateral distance  $l$  is 0.8 cm. Cathode layers with Faraday dark space are clearly visible in Figure 9 whereas they were hidden by the halo in Figure 8.

The effect of merging into one discharge column can be explained as follows. When the discharges become sufficiently close from one another, the volume of gas between the two discharges heats up. The gas density decreases, and therefore the reduced field strength  $E/N$  increases. The  $E/N$  increase may also occur partially due to a higher electric field in the discharge interspace. The relative effects of gas heating and higher electric field remain to be elucidated. Since

$E/N$  is proportional to the electron temperature, the region between the discharges undergoes more intense ionization processes. Thus a preferential channel develops in the space between the two discharges, thereby leading to the X-shape.

#### **4.2. Dual-Discharges in a Fast Preheated Air Flow**

The photographs presented in Figure 10 show a dual DC discharge in atmospheric pressure air preheated to  $T \sim 2000$  K. The electrode configuration is the same as for dual discharges in ambient air (cathodes at the bottom, anodes at the top). Preheated air is injected into the discharge from the bottom at flow velocities from ~25 to ~160 m/s. The interelectrode distance is 1 cm, and the lateral distance between the two discharges is 0.5 cm. In all cases, the total current is 200 mA, with ~100 mA per single discharge. The voltage across the discharge gap varies from 1.22 kV at 25 m/s to 2.1 kV at 160 m/s.

The two discharges do not interact in the same way as in the slow flow of ambient air. In particular, the two columns have less of a tendency to merge into an X-shape discharge. The merging effect in ambient air is, as explained in the previous section, likely due to gas heating in the space between two discharge columns. This effect does not occur in the fast air flows because the residence time of the gas between the electrodes is too short for collisional relaxation of vibrationally excited  $\text{N}_2$  molecules.

One can notice the formation of a large luminous halo above the anodes on the vertical axis, especially in the 25 m/s flow. This halo is caused by emission from  $\text{NO}_2$  in the air heated by the discharge, as already observed in our discharges with ambient air. The discharges are less spatially and temporally homogeneous at high flow velocities, as can be seen in the high velocity case (Figure 10b) where plasma filaments appear. However, filamentation occurs at the (cold) edges of the preheated flow, and is less likely to appear in a uniform preheated flow.

This approach shows that the plasma volume can be increased by the operation of dual or multiple DC discharges.

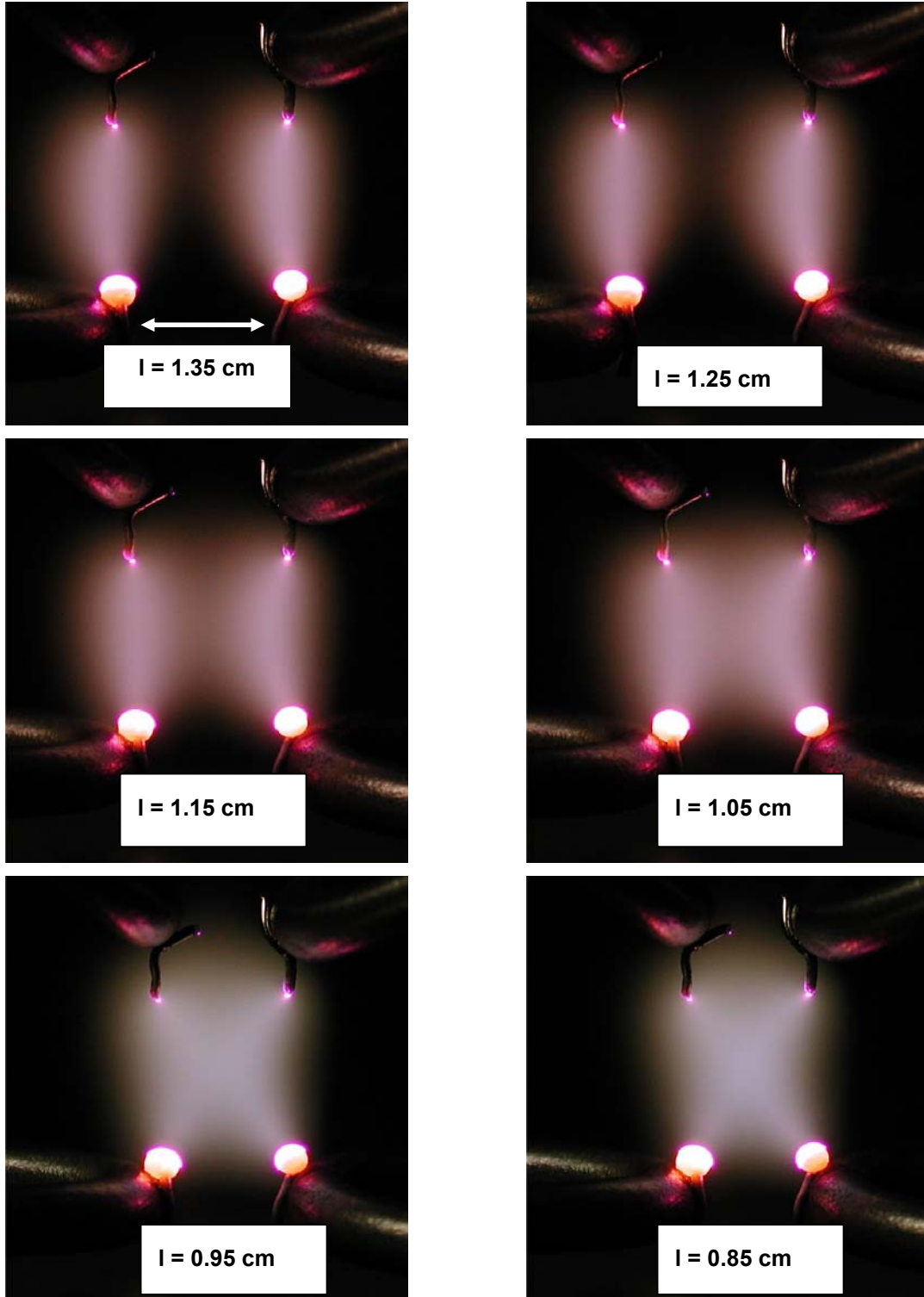


**Figure 8.** Dual discharges in ambient air at atmospheric pressure for various separation between discharges. The interelectrode distance 1.2 cm, gas velocity 50 cm/s, current 100 mA and voltage 1.4 kV per single discharge.

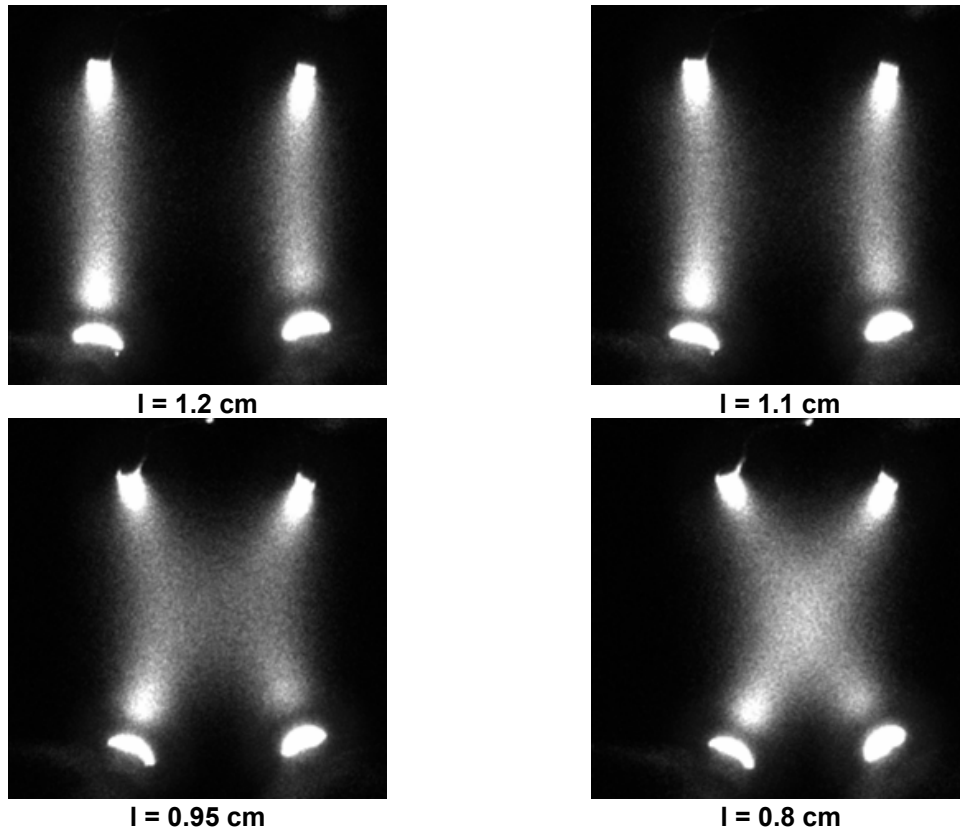
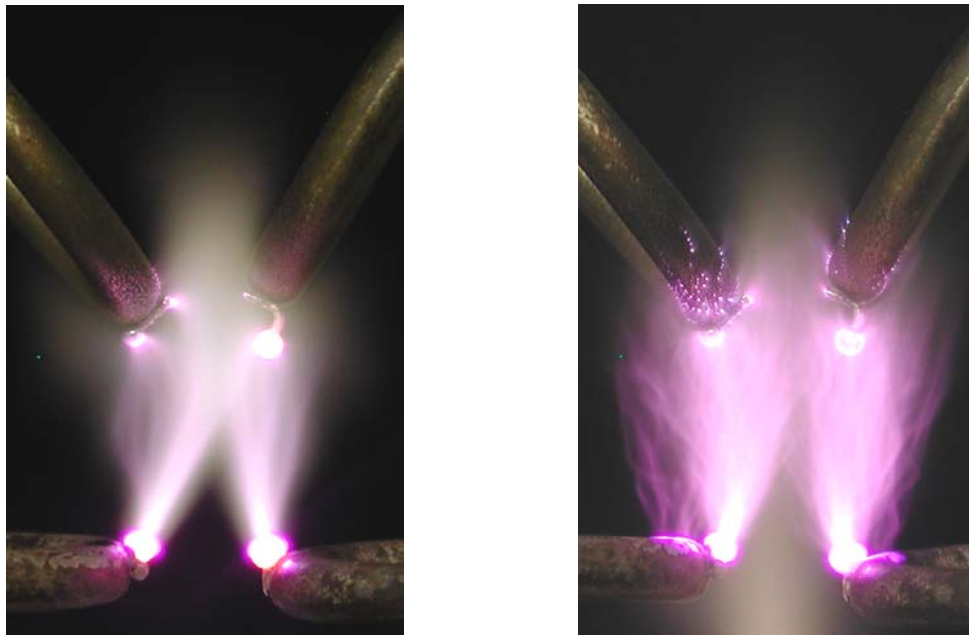


Figure 9. Spectral distribution of the emission intensity of the  $N_2$  C-B (0,0) head band at 337 nm. Gas velocity, current and voltage are the same as for Figure 8.



a)  $Q = 17$  slpm,  $v \approx 25$  m/s,  $U_d = 1.22$  kV

b)  $Q = 110$  slpm,  $v \approx 160$  m/s,  $U_d = 2.1$  kV

Figure 10. Dual discharge in air flow preheated to  $\sim 2000$  K. Current 200 mA (total), interelectrode spacing 1 cm, lateral distance between discharges 0.5 cm.

## 5. Multiple Repetitively Pulsed Discharges in Preheated Air

As discussed in section 3.3, repetitively pulsed discharges with short (10 ns) high voltage (10 kV) pulses represent a novel method to efficiently produce electron densities of about  $10^{12} \text{ cm}^{-3}$ . The power requirements are two to three orders of magnitude lower than for DC discharges producing the same electron density. Additionally, these discharges produce no noticeable electrode erosion

Parallel operation with six sets of electrodes has been demonstrated in atmospheric pressure air preheated to  $\sim 2000 \text{ K}$ . The experiment is shown in Figure 11. Preheated air flows at about 10 m/s from bottom to top. The parallel pulsed discharges are easier to implement than DC discharges because they do not require individual ballasting on each pin. Furthermore, the discharges do not merge into a single column, unlike the dual DC discharges in ambient air, because the temperature of the air flow remains uniform. In the pulsed discharges, Joule heating of the gas is very low because the overall discharge power is two to three orders of magnitude lower than in the DC discharges. Thus the gas density is approximately uniform in the entire volume of the multiple discharges, and the reduced field strength  $E/N$  which controls ionization, is essentially a function of  $E$ . We have achieved a plasma volume of about  $0.5 \text{ cm}^3$ . Scaling to larger volumes can be done with additional pins.



**Figure 11. Multi-pin repetitively pulsed discharge in preheated ( $\sim 2000 \text{ K}$ ), atmospheric pressure air. Discharge volume  $\sim 0.5 \text{ cm}^3$ . Electron number density:  $\sim 10^{12} \text{ cm}^{-3}$ .**

## 6. Transverse DC Discharges in Preheated Air Flow

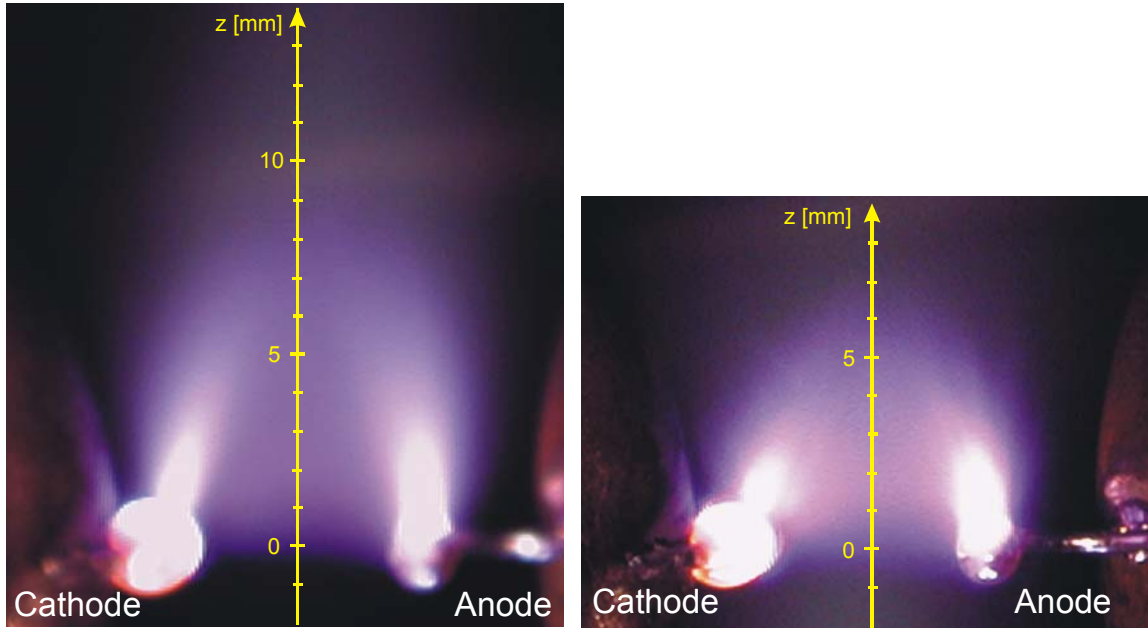
In the previous sections of this paper, the electrical discharges were applied along the axis of the gas flow. We now describe experiments with a DC discharge perpendicular to the axis of the flow. Two flow velocity conditions are investigated. We find that the slower flow “blows out” the discharge farther than the faster flow. To explain this counterintuitive result, we have made measurements of gas temperature and electric field profiles in the discharge, and we propose an explanation of the observed behavior based on the measured reduced field strength  $E/N$  in the discharge region.

### 6.1. Single DC Discharge in Transverse Air Flow

The experiments presented here were conducted for two flow rate conditions, 32 and 110 slpm. The corresponding flow velocities are about 45 and 160 m/s. In both cases, the air flow was preheated to  $\sim 2000 \text{ K}$  with the microwave plasma torch. The DC discharge is applied between two platinum pins orthogonal to the axis of the flow. The electric circuit is the same as for the single DC discharge experiments presented earlier (Figure 2).

Figure 12 shows photographs of the transverse discharges for the slow (Figure 12a) and fast (Figure 12b) flow conditions. In both cases the inlet gas temperature is approximately 2000 K, the interelectrode spacing 5 mm, the discharge current 100 mA. The voltage difference between the two electrodes is 1.2 and 1.33 kV for the gas flow rates of 32 and 110 slpm, respectively. The discharge volume is visually larger at the low flow rate condition. This observation may be somewhat paradoxical because one would expect the fast flow to blow the discharge farther downstream than the slow flow. Figure 13 shows the measured intensity profiles of  $\text{N}_2 \text{ C-B } (0,0)$  emission along the centerline axis of the flow. These profiles confirm that the discharge extends farther downstream at low flow rate. They also show that the peak of  $\text{N}_2$  emission is less intense in the slow flow than in the fast flow.

We anticipate that the observed emission profiles correlate with the reduced field strength profiles  $E/N$ . This is because the reduced field strength is the main parameter controlling the rate of electron-impact reactions. We obtained  $E/N$  from measurements of the electric field and gas temperature (from which we infer the gas density  $N$ ) along the centerline axis of the flow.



a)  $Q = 32$  slpm,  $v \sim 45$  m/s,  $U_d = 1.2$  kV

b)  $Q = 110$  slpm,  $v \sim 160$  m/s  $U_d = 1.33$  kV

**Figure 12. Transverse DC discharge in preheated air flow. Flow direction: vertical upward. Interelectrode spacing: 5 mm, gas temperature:  $\sim 2000$  K, discharge current: 100 mA.**

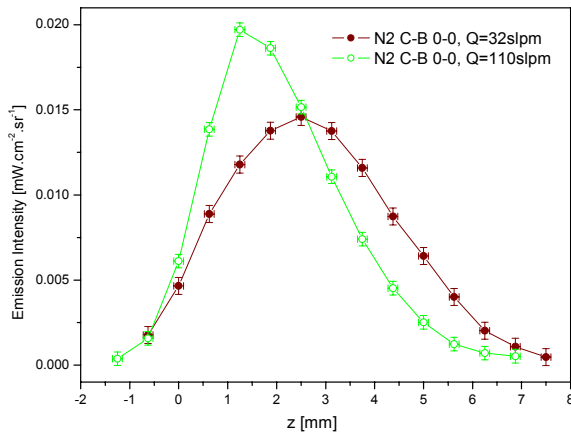


**Figure 13. Emission intensity profiles of N2 C-B (0,0) along vertical transverse discharge axis.**

### Electric field measurement

We measured the electric potential along the centerline  $z$ -axis of the flow with a high voltage probe connected to a platinum wire placed inside a ceramic tube (Figure 14a). To determine the electric field strength from the measured floating potential, we make the following approximations:

- Since the discharge forms an arch, we assume that the current streamlines form arches as well. The length of an arch  $d$  is approximated by the length of the straight line between the cathode surface and the probe pin on the vertical axis, i.e.  $d^2 = (2.5 \text{ mm})^2 + z^2$ .
- We assume that the electric field is constant along a current streamline. This approximation only holds in the positive column and not in the cathode layer but the cathode layer is much thinner than the positive column.

With these approximations, the electric field is calculated as the measured floating potential of the probe minus the cathode potential fall, divided by the length  $d$  of the arch extending from the surface of the (grounded) cathode pin to the probe (Figure 14b). We are working on a more accurate technique of measuring  $E$ , using a double probe which measures the potential difference at a fixed spacing. Preliminary results agree with the single probe measurements.

The electric field profiles measured for the two flow rate conditions are shown in Figure 15. Their shapes are similar, although in the low flow rate case the maximum  $E$  is shifted a little further downstream and the  $E$  magnitude is about 30% smaller. This difference can be partly explained by noting that the voltage across the gap is smaller in the low flow rate case (1.2 kV vs. 1.33 kV). This reason is however insuffi-

cient to completely explain the differences in the field profiles, and further work is required to better understand this effect.

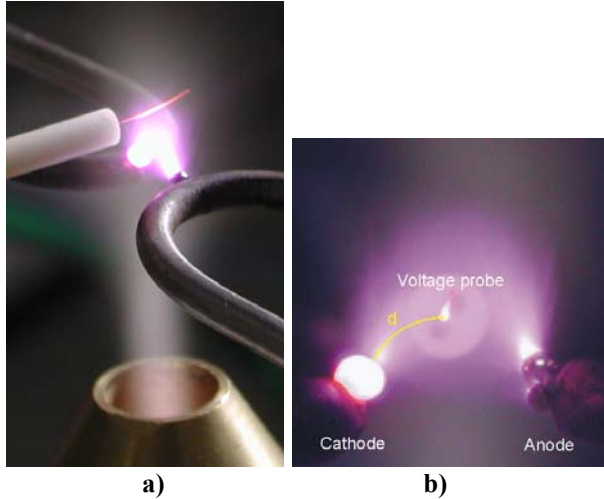


**Figure 14.** Experimental setup for electric field measurements along the centerline axis of the flow. a) Overview of the setup: microwave nozzle, preheated air plasma flow, stainless-steel tubes with pin electrodes, discharge, and voltage probe. b) side view of the set-up: pin electrodes, discharge, voltage probe, and current streamline from the cathode to the probe.

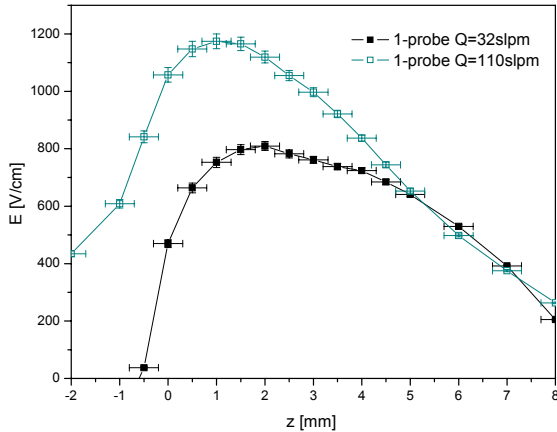


**Figure 15.** Measured electric field profiles in the transverse discharges.

### Gas density measurement

We obtain the gas density profile from the gas temperature profile through the state equation  $N = p/kT$ . The gas temperature is assumed to be equal to the rotational temperature, measured from the shape of the

bands of the  $N_2$  C-B emission. The measured profiles, shown in Figure 16, indicate that the gas temperature increases more in the slow flow than in the fast flow, even though the total power dissipated in the discharge is a little higher in the fast flow case (133 W vs 120 W at slow flow). This effect can be explained again in terms of VT transfer (see section 3.2). In both cases, the discharge excites the vibrational modes of  $N_2$  which then relax through collisions. This collisional quenching transfers energy from vibration into the translational modes of molecules, thereby heating the gas. There is more gas heating at low flow rate (i.e. low flow velocity) because the vibrational modes have more time to relax when the residence time is longer. This explains why the temperature increases more in the low flow rate case.

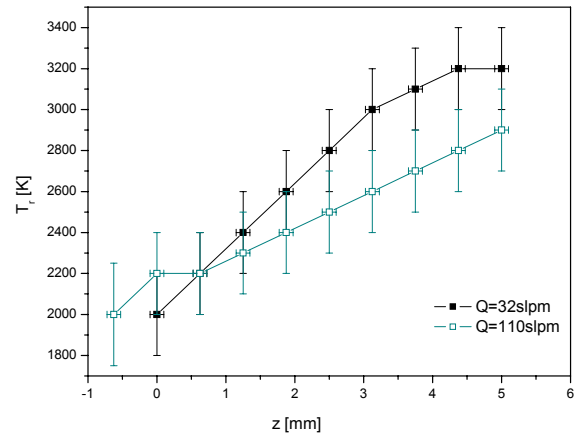


**Figure 16.** Rotational temperature profiles in the transverse discharges.

### Reduced electric field strength

The reduced field strength  $E/N$  profiles deduced from the measured electric field and gas density profiles is shown in Figure 17. In Figure 18, we compare the  $E/N$  profiles with the optical emission profiles of the  $N_2$  C-B (0,0) band from Figure 13. The  $E/N$  and emission profiles correlate well. It should be mentioned that small changes of  $E/N$  cause large changes of emission intensity.

The results of the approximate measurements of  $E/N$  confirm that the extent of the discharge correlates with the reduced field strength profile. The  $E$  component of  $E/N$  itself slightly depends on the flow conditions, this is a subject of further investigation. However, the paradoxical wider extent of the discharge at low flow velocities appears to be mainly caused by a higher temperature downstream. Higher temperature results in lower gas density, thereby increasing the  $E/N$  further downstream.

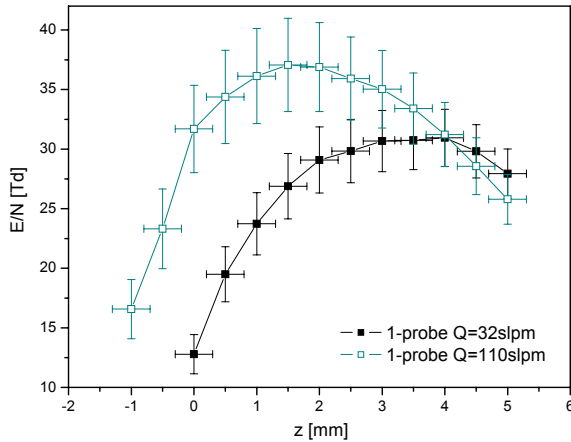


**Figure 17. Measured reduced field strength ( $E/N$ ) profile in the transverse discharges.**

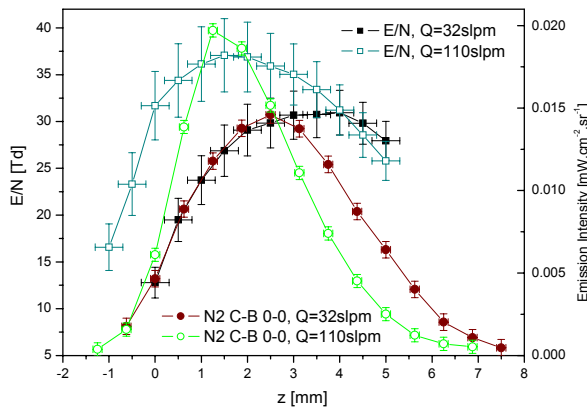


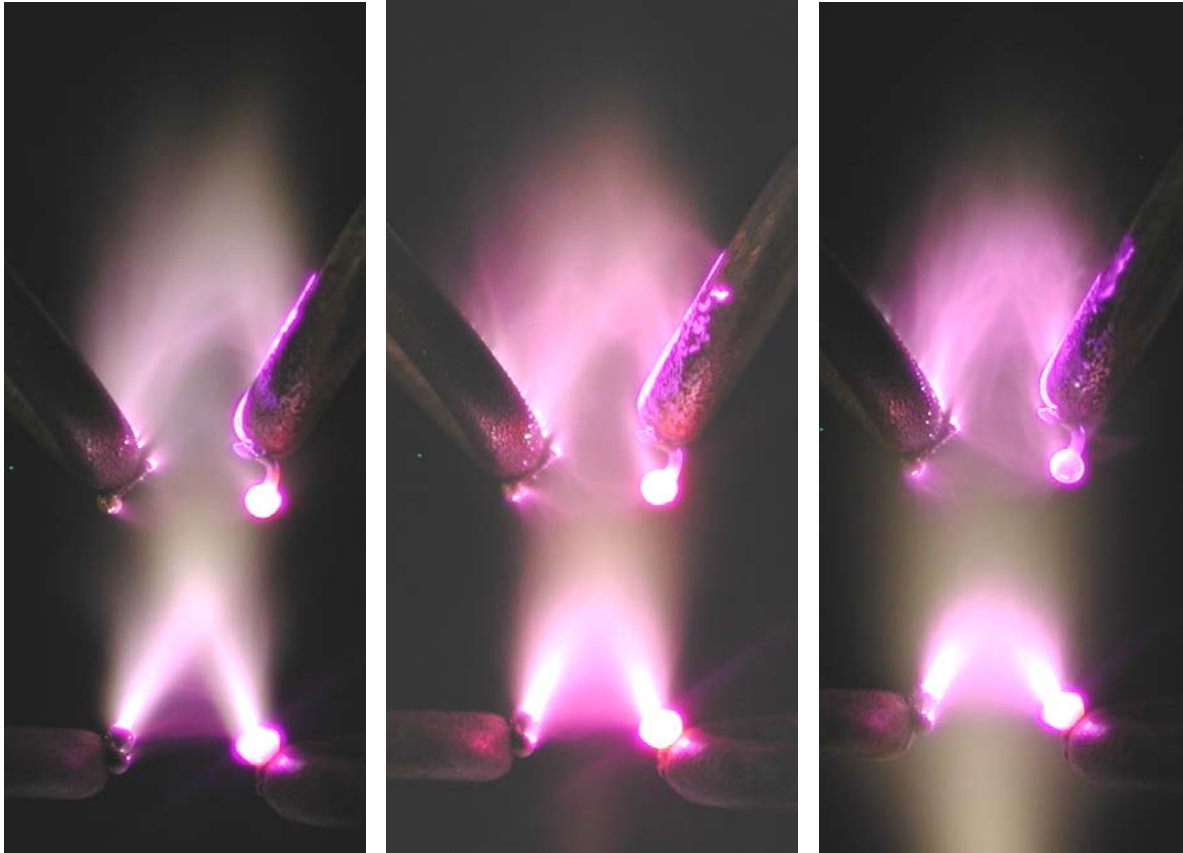
**Figure 18. Comparison of  $E/N$  profiles and  $N_2$  C-B (0,0) emission profiles in the transverse discharges.**

## 6.2. Dual DC Discharge in Transverse Air Flow

The results of experiments with transverse discharges led us to conduct experiments with dual discharges in transverse flow of air preheated to  $\sim 2000$  K. The photographs presented in Figure 19 show the discharge configuration (cathodes on the right, anodes on the left). The preheated air is injected into the discharge from the bottom perpendicularly to the discharge axis, at various gas flow rates (17-110 slpm) corresponding to flow velocities from  $\sim 25$  to  $\sim 160$  m/s. The interelectrode spacing is 0.5 cm, and the lateral (vertical) distance between the two discharges is 1 cm. In all cases, the total current is 200 mA, with  $\sim 100$  mA per single discharge.

As can be seen from Figure 19, the lower discharge is very similar to the single discharge in transverse flow. On the other hand, the upper discharge looks different, the plasma spreads to the volume along the electrodes. The differences between the lower and upper discharges are due to different air flow properties and temperature patterns. The temperature and flow velocity tend to decrease along the vertical axis. On the other hand, the lower discharge dissipates a certain amount of energy into the flow. This effect is stronger at low flow velocities (25 m/s) where the lower discharge almost reaches the upper discharge. The discharges look more diffuse and spatially homogeneous at low flow velocities, similar to dual discharges in parallel flow (section 4.3.).

Dual or multiple DC discharges in either parallel or transverse air flow represent possible ways to obtain larger volumes of atmospheric pressure air plasmas.



a)  $Q = 17$  slpm,  $v \approx 25$  m/s

b)  $Q = 32$  slpm,  $v \approx 45$  m/s

c)  $Q = 110$  slpm,  $v \approx 160$  m/s

Figure 19. Dual discharge in transverse air flow preheated to  $\sim 2000$  K.  $I = 200$  mA (total), interelectrode spacing 0.5 cm, vertical distance between discharges 1 cm.

## 6. Conclusions

We have presented an experimental study of the scalability of DC and repetitively pulsed glow discharges in ambient and preheated air at atmospheric pressure. The objective was to scale up the plasma volume while keeping the electron number density of at least  $10^{12}$   $\text{cm}^{-3}$  and the gas temperature at or below 2000 K.

Repetitively pulsed discharges represent an alternative to DC discharges, generating the same electron densities at considerably lower power requirements (250 times lower to sustain  $10^{12}$  electrons/ $\text{cm}^3$  than with a DC discharge). This is because a large amount of the electron energy in the DC discharges is lost via excitation of vibrational modes of molecules (mainly  $\text{N}_2$ ). In the pulsed discharges the electron energy is used more effectively during the very short pulse, there is less time for VT transfer and subsequent gas heating. The effect of gas heating can be also sup-

pressed by applying the DC discharges in fast flows of preheated gas. The vibrational modes of  $\text{N}_2$  have less time to relax in the fast flow, hence cannot heat the gas as much as in the slow flow. The temperature in the discharge is then essentially determined by the inlet gas.

Single DC discharges can produce plasma volumes of up to  $0.5$   $\text{cm}^3$ . We have shown that this volume can be doubled with a dual-discharge facility. For a given gas flow velocity, there is a minimum interdischarge distance below which the discharges merge into a single column of nearly twice the diameter of the single discharge. Formation of a single column is due to enhanced gas heating in the space between the two columns resulting in enhanced reduced field strength  $E/N$ . Since  $E/N$  is proportional to the electron temperature, the region between the discharges undergoes more intense ionization processes. Thus a preferential channel develops in the space between the two discharges, leading to the X-shape aspect.

The shape of dual DC discharges in preheated air depends on the flow velocity which controls the rate of gas heating. The dual discharges in fast flows (160 m/s) do not merge into one column because there is little heating of the air in the space between them.

Repetitively pulsed discharges have been scaled up by using a multiple-pin configuration. A plasma volume of about  $0.5 \text{ cm}^3$  was formed with very low power requirements by using six elementary discharges in parallel. Larger volumes can be achieved by increasing the number of elementary discharges.

Finally, the study of DC discharges in transverse air flow has shown interesting and somewhat paradoxical effects. The discharge extends further at low flow velocity than at high flow velocity. The vertical extent of the discharge is controlled by the axial profile of the reduced field  $E/N$ . It appears that the discharges in transverse flow behave counter-intuitively because of the higher temperature increase downstream at low flow velocity. Higher temperature results in lower gas density, thereby increasing  $E/N$  further downstream the flow. Two transverse discharges placed one above another enable to produce plasma volumes comparable to those obtained with dual discharges in parallel flow.

Dual and multiple discharges represent a promising way for scaled-up nonequilibrium plasmas. These studies, and especially the transverse flow experiments, show that the flow velocity, which determines the level of gas heating, has an important effect on the plasma properties. This effect should be considered when designing further scaled-up plasmas.

### **Acknowledgements**

This work was funded by the Director of Defense Research & Engineering (DDR&E) and by the Air Force Office of Scientific Research under the cognizance of Dr. Robert J. Barker (Grants AF-F49620-97-1-0316 and F49620-01-1-0389). We gratefully acknowledge LITMAS, Inc. for loaning us the Litmas Red microwave torch.

### **References**

[1] R.J. Gessman, C.O. Laux and C.H. Kruger, "Kinetic Mechanisms of Recombining Atmospheric Pressure Air Plasmas," AIAA 97-2364, 28<sup>th</sup> AIAA Plasmadynamics and Lasers Conference, Atlanta, GA, June 23-25, 1997

[2] C. O. Laux, R. J. Gessman, D. M. Packan, L. Yu, C. H. Kruger, and R. N. Zare, "Experimental Investigations of Ionizational Nonequilibrium in Atmospheric Pressure Air Plasmas," 25<sup>th</sup> IEEE International Conference on Plasma Science (ICOPS), Raleigh, NC, 1998.

[3] C. O. Laux, L. Yu, D. M. Packan, R. J. Gessman, L. Pierrot, C. H. Kruger, and R. N. Zare, "Ionization Mechanisms in Two-Temperature Air Plasmas," 30<sup>th</sup> AIAA Plasmadynamics and Lasers Conference, Norfolk, VA, 1999.

[4] M. Nagulapally, G. V. Candler, C. O. Laux, L. Yu, D. Packan, C. H. Kruger, R. Stark, and K. H. Schoenbach, "Experiments and Simulations of DC and Pulsed Discharges in Air Plasmas," 31<sup>st</sup> AIAA Plasmadynamics and Lasers Conference, Denver, CO, 2000.

[5] L. Yu, L. Pierrot, C. O. Laux, and C. H. Kruger, "Effects of Vibrational Nonequilibrium on the Chemistry of Two-Temperature Nitrogen Plasmas," *Plasma Chemistry and Plasma Processing*, vol. 21, pp. 483-503, 2001.

[6] L. Yu, C. O. Laux, D. M. Packan, and C. H. Kruger, "Direct-Current Glow Discharges in Atmospheric Pressure Air Plasmas," *J. Appl. Phys.*, vol. 91, pp. 2678-2686, 2002.

[7] C. H. Kruger, C. O. Laux, L. Yu, D. M. Packan, and L. Pierrot, "Nonequilibrium Discharges in Air and Nitrogen Plasmas at Atmospheric Pressure," *Pure and Applied Chemistry*, vol. 74, pp. 337-347, 2002.

[8] X. Duten, D. Packan, L. Yu, C. O. Laux, and C. H. Kruger, "DC and Pulsed Glow Discharges in Atmospheric Pressure Air and Nitrogen," *IEEE Transactions on Plasma Science Special Issue on "Images in Plasma Science"*, vol. 30, pp. 178-179, 2002.

[9] D. Packan, L. Yu, C. O. Laux, and C. H. Kruger, "Repetitively-Pulsed DC Glow Discharge in Atmospheric Pressure Air: Modeling and Experiments with a 12 kV, 10 ns, 100 kHz Pulse Generator," 28<sup>th</sup> IEEE International Conference on Plasma Science, Las Vegas, NV, 2001.

[10] D. M. Packan, "Repetitively Pulsed Glow Discharge in Atmospheric Pressure Air," Ph.D. Thesis, *Mechanical Engineering*. Stanford, CA: Stanford University, 2002.

- [11] A. P. Yalin, C. O. Laux, C. H. Kruger, and R. N. Zare, "Spatial Profiles of  $N_2^+$  Concentration in an Atmospheric Pressure Nitrogen Glow Discharge," *Plasma Sources Science and Technology*, vol. 11, pp. 248-253, 2002.
- [12] L. Yu, D. M. Packan, C. O. Laux, and C. H. Kruger, "Direct-Current Glow Discharges in Atmospheric Pressure Air and Nitrogen Plasmas," 28<sup>th</sup> IEEE International Conference on Plasma Science, Las Vegas, NV, 2001.
- [13] E. E. Kunhardt, *IEEE Trans. Plasma Sci.* vol. 28, pp. 189-200, 2000
- [14] A.-A. H. Mohamed, R. Block, K. H. Schoenbach, *IEEE Transactions on Plasma Science Special Issue on "Images in Plasma Science"*, vol. 30, pp. 182-183, 2002.
- [15] R. H. Stark and K. H. Schoenbach, *Appl. Phys. Lett.*, vol. 74, pp. 3770-3772, 1999
- [16] R. H. Stark and K. H. Schoenbach, *J. Appl. Phys.*, vol. 89, pp. 3568-3572, 2001
- [17] Z. Machala, „Continuous and transient electrical discharges, streamer triggered, at atmospheric pressure, for the removal of Volatile Organic Compounds (VOC)”, Ph.D. thesis, University Paris-Sud XI, France; Comenius University, Slovakia, 2000
- [18] O. Goossens, T. Callebaut, Yu. Akishev, A. Napartovich, N. Trushkin, C. Leys, *IEEE Transactions on Plasma Science Special Issue on "Images in Plasma Science"*, vol. 30, pp. 176-177, 2002.
- [19] C. O. Laux, "Optical Diagnostics and Radiative Emission of Air Plasmas," Ph.D. Thesis, *Mechanical Engineering*. Stanford, CA: Stanford University, 1993.
- [20] Y. P. Raizer, "Gas Discharge Physics." New York: Springer, 1991, pp. 278-279.